1D Interferometric Rayleigh scattering velocimetry and thermometry using VIPA

Xinguang Luo, Zeinab Al Hadi, Yedhu Krishna, Gaetano Magnotti*
Clean Combustion Research Center, King Abdullah University of Science and Technology, Saudi Arabia
* Correspondent author: gaetano.magnotti@kaust.edu.sa

Keywords: Interferometric Rayleigh scattering, VIPA, velocimetry, thermometry

ABSTRACT

One-dimensional interferometric Rayleigh scattering is applied to simultaneous measure velocity and temperature by using virtually imaged phased array. The Doppler shift of interferometric pattern was produced by flow velocity plus laser drifts. Online monitoring of the laser wavelength is achieved by adding an additional F-P etalon-based IRS system. Velocity measurements at a low flow rates show an accuracy of 10 m/s. The Rayleigh-Brillouin spectrum is function of pressure and temperature, and provides temperature diagnostics in isobaric flows. The different fringes of interferometric pattern represent different measurements in temperature fitting. This make it possible that one-time experiment but multi-times measurement. The instrument precision of temperature was 3.5% at 809K, which was contributed by the signal to noise ratio decrease at high temperature.

1. Introduction

Measurement of velocity and temperature of a reaction or non-reaction flow is extremely important in combustion and aerospace community to improve the understanding of the flow's fundamental mechanism and validate the Computational Fluid Dynamics(CFD) model. There are a lot of techniques developed in this field such as particle image velocimetry(PIV), molecular tagger velocimetry(MTV) for velocity measurement and thermocouple for temperature measurement. However, those techniques would become quite complex when applied into harsh combustion environment such as pre-chamber and gas turbine, in which the particle tracer or the invasive instrument would affect the flow or the combustion. Therefore, Laser-based technique is promising way to do measurement in cruel environment. And Interferometric Rayleigh scattering(IRS) is a typical example of laser-based technique to measure velocity and temperature in tracer-free and noninvasive.

Conventionally in IRS (Panda & Seasholtz, 1999; Seasholtz, 1995), the Rayleigh scattering signal generated at the probe volume is sent through a Fabry-Perot (FP) etalon, to generate an interference fringe pattern, imaged on a camera. If the flow has a velocity component in either the direction of the laser beam or of the collection optics axis, then the fringe pattern will be Doppler shifted, by an amount proportional to the velocity. In addition, the Rayleigh-Brillouin

spectrum is function of pressure and temperature, and provides temperature diagnostics in isobaric flows (Boley, Desai, & Tenti, 1972). The technique has been applied to several high-speed flows, and extended to kHz sampling rate using a pulse-burst laser, but it is inherently a 0D or multi-point technique (Cutler, Rein, Roy, Danehy, & Jiang, 2020). Recently, by replacing the etalon with a virtually imaged phase arrays (VIPA), we have extended the technique to 1D velocity measurements (Krishna, Luo, & Magnotti, 2021). In this work, we introduce an improved 1D VIPA system, featuring an online monitoring of the laser wavelength, and we demonstrate for the first time simultaneous IRS 1D measurements of temperature and one component of velocity.

Online monitoring of the laser wavelength is essential for accurate and precise velocity measurements. A simple approach (Bivolaru, Danehy, Lee, Gaffney, & Cutler, 2006; Estevadeordal et al., 2018; Sheng et al., 2017) is to send a portion of the laser to a scattering plate and to record the interference pattern. In the previous 1D IRS velocimetry demonstration using the VIPA in place of the etalon, the Rayleigh and reference signals were not taken simultaneously, which assumes that the laser frequency does not change significantly during the time period between subsequent images. The current work overcomes this limitation by adding an additional F-P etalon-based IRS system to monitor the change in the laser wavelength. The improved instrument is then applied to an electrically heated jet issuing from a contoured converging nozzle to generate high velocity flow at elevated temperatures.

2. Experiment setup

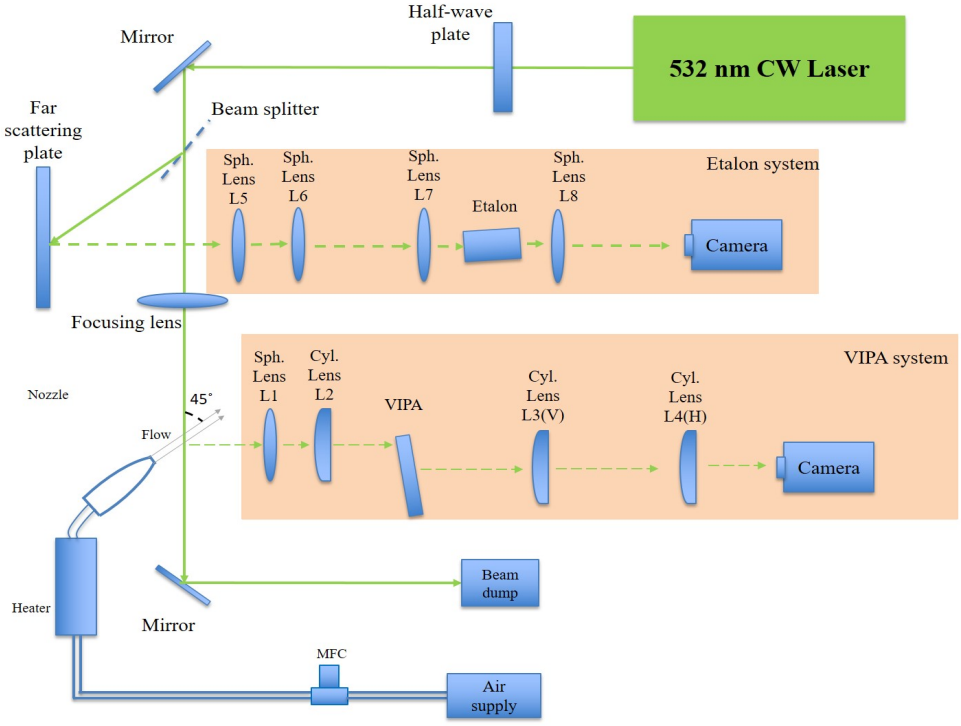

Figure 1. Schematic of experimental setup

A schematic of the experimental setup is shown in figure 1. A 3.5 KW electric flow heater is used to heat the flow to elevated temperature. This heater applies PID control by using a thermocouple insert inside the heater to detect the flow temperature. In experiment, there is another thermocouple placed at the exit of the nozzle the measure the flow temperature.
This experiment uses one CW 532 nm laser running at 2W as the light source. A half-wave plate rotates the laser polarization from horizontal to vertical to maximize the Rayleigh scattering efficiency. A 90/10 beam splitter reflects 10% of laser energy to a far scattering plate; 90% of laser beam is focused to the measurement volume by a 300 mm focal length (f.l.) lens and then it is redirected to a beam dump. The 1D IRS system employs a VIPA designed for operation in the 500 nm-600 nm range and with a 15 GHz free spectral range (FSR). The collection optics for the VIPA system consist of a spherical lens (200 mm f.l.) to collimate the Rayleigh signal, a 150 mm f.l. cylindrical lens to focus the signal along a line at the back surface of the VIPA entrance, and two cylindrical lenses (L3, 750 mm f.l. and L4 300 mm f.l.) to focus the 1D interferometric pattern on the EMCCD camera. Cylindrical lens L3 and L4 are placed separately in vertically and horizontally direction. The focal length of L3 determines the number of fringes appearing on the camera, and the spectral resolution of the instrument. L4 determines the spatial magnification. To improve the signal-to-noise ratio (SNR), the camera is hardware binned by 4 pixels in the spatial direction leading to one super-pixel corresponding to 31μm in physical space. To avoid the bowing effect introduced by L1, only the central 71 rows are used in data analysis, which gives 2.2 mm length for the 1D detection region. There is no binning in the spectral direction to maximize the spectral resolution. The etalon system, works in parallel with the VIPA, imaging the reference interferogram from the scattering place. The etalon is a 1" diameter, air-spaced FP etalon with a FSR of 30 GHz, and AR coated for the 530 nm to 660 nm range. The collection optics consist of a 150 mm f.l. spherical lens (L5) to collect and collimate the scattering light from the scattering plate, a telescope consisting of a 300 mm f.l. spherical lens (L6) and a 100 mm spherical lens (L7) to reduce the diameter of the collimated signal so that it can travel through the 1-inch etalon, and a 300 mm f.l. spherical lens to image the interferogram on an EMCCD camera.
The left image in Figure. 2 shows image of interferogram in the VIPA side. The camera was hardware binned 4 pixel in spactial direction to increase signal to noise ratio, the super pixel resolution was 31μm. The length of test region field was 2.2mm which results 77 measurements point. The left image in Figure. 2 shows the image of interferogram in the Etalon side. The camera was also hardware binned 4 pixel to synchronize with VIPA side camera. The useful field of view is picked as 2.2mm to correct the laser wavelength change during exposure time. The exposure

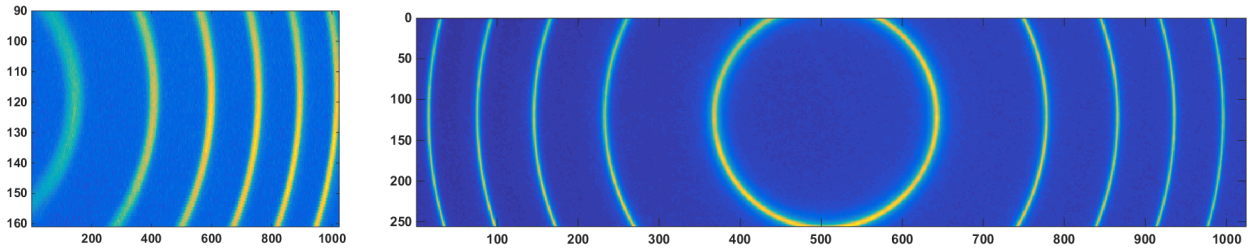

(a) (b)

Figure 2. (a) VIPA interferometric pattern (b) Etalon interferometric pattern

time of two camera set as 1s. The measurements are 1D, the whole view of filed is 7.9mm. Due to the bowing effect in the image, only the central 2.2mm data was used in data analysis.

Both VIPA and Etalon side data are denoised using a wavelet adaptive thresholding and reconstruction algorithm. Then all images are transformed from spectrum space into frequency space accroding to the pixel locations of the peak of the fringes. The free spectral range(FSR) is 15 GHz in VIPA and 30GHz in Etalon. By using a least square curvefit algorithm, the frequency variation between no-flow and flow fringes can be obtained. Measuring temperature requires first the determination of the instrument function. This is obtained by deconvolution of room temperature data with the theoretical Rayleigh Brillouin spectrum obtained from the Tenti S6 model. Then a database of RBS profiles is developed by convolving the instrument function with RBS Tenti S6 model at different temperatures. This database is used to obtain the temperature by comparison against the experiment data. Gaussian fitting is applied to find the center of each scattering fringes. The frequency variation with time can be exported and used to calibrate the velocity measurement.

3. Results and discussion

3.1 Temperature measurement

In temperature measurement, the contoured converging nozzle is removed. The temperature of heater setting varied from 300K to 1000K with a 50K gap. The thermocouple was placed at 12.7mm away from the heater exit. For each temperature setting, record VIPA image after the thermocouple reading is stable.

In this work, a series of theoretical Rayleigh-Brillouin scattering spectrum from 270K to 1000K with a 5K gap is generated by Tenti S6 model. The instrument function is produced by fitting VIPA experiment spectrum with theoretical spectra convoluted flexible parameter voigt function. Deconvolution experiment data at different temperature with this voigt shape instrument function to generate experiment 'Rayleigh-Brillouin' shape profile. A least square algorithm is used between experiment 'Rayleigh-Brillouin' shape and theoretical spectrum to get the best fitted temperature. Figure.3 shows the experiment results of no flow, room temperature condition with flow and high temperature condition. The tempearture plays a role in signal intensity and broadening. And the velocity of the flow would result the shift of the whole pattern.

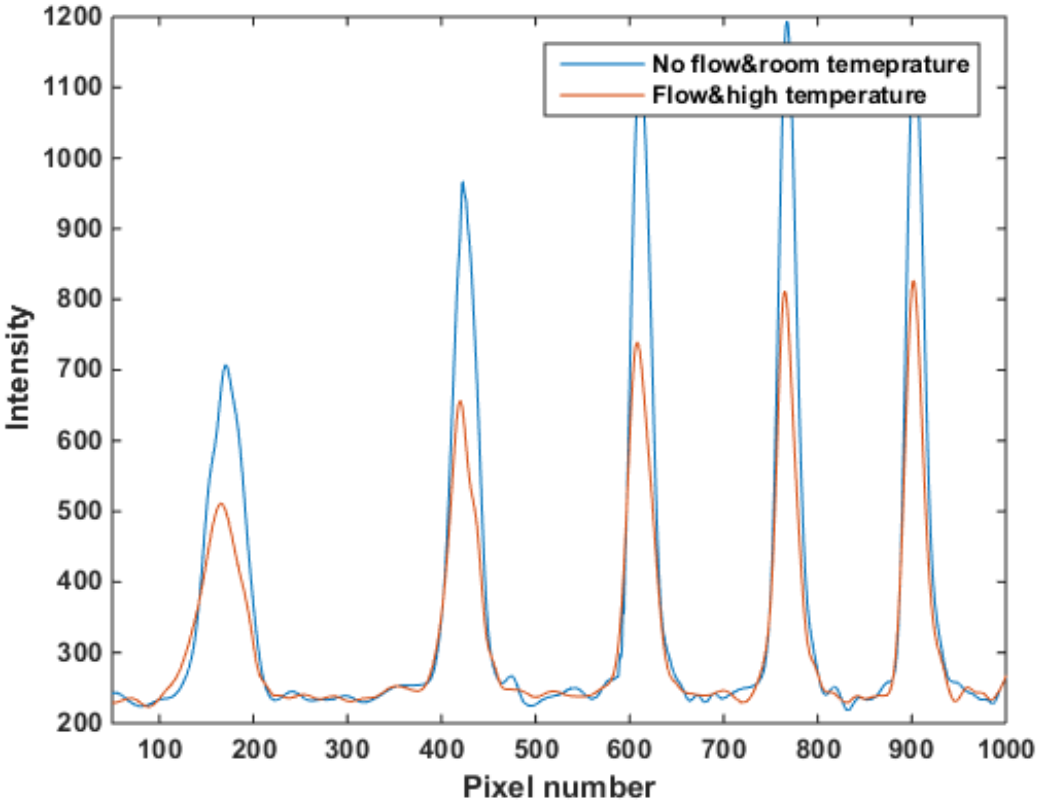

Figure 3. Typical spectra of experiment results

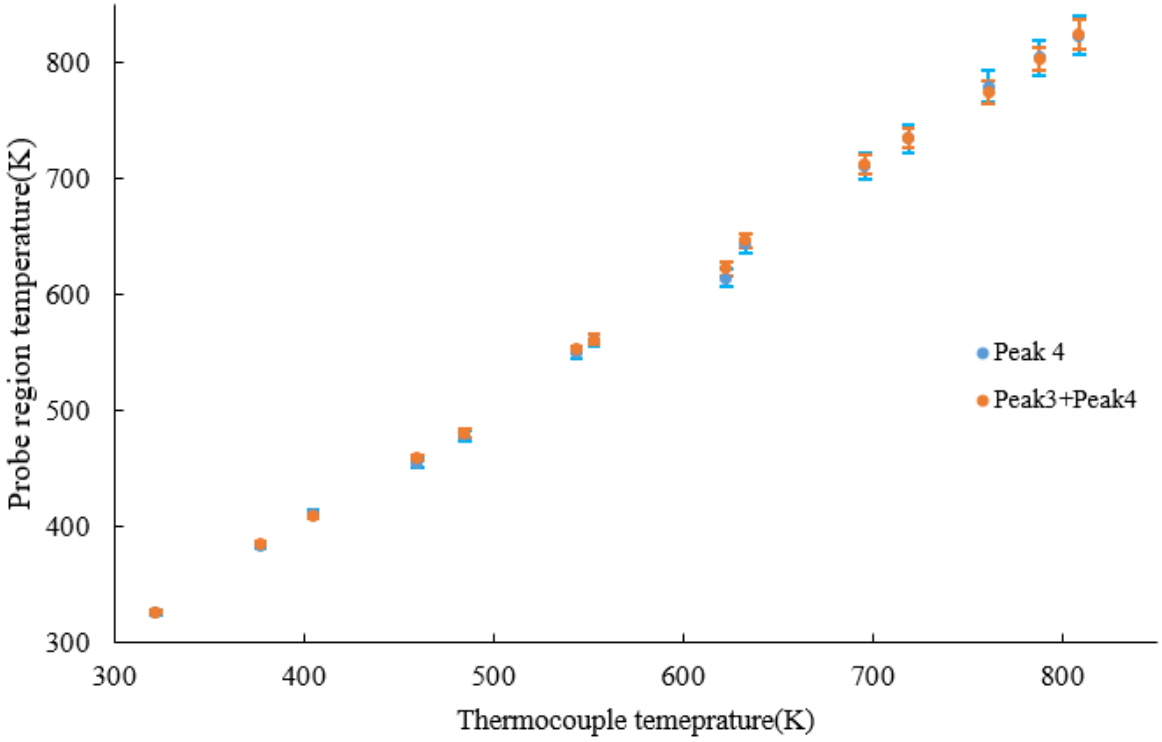

Figure.4 Measurements of the region temperature

Figure.4 compared results from the thermocouple at the exit and the temperature from the fitting. The discrepancy is smaller than 4%. The error bar in Figure.4 represent the stand diviation of the fitting result. As the flow temperature increase, the std of fitting also increase. If only considering peak 4 to d otemperature fitting, the maximum std of the temperature is 4.4% at 809K. If take peak 3 and peak 5 into consideration, the std of the temperature would decreace to 3.5%. The std of this fitting could improve by counting two peaks in interferometric pattern. this feature represents that each peak of data actually is an independant temperature measurement. Hence the number of fringers also could be regarded as the number of measurements in one interferometic pattern. And the std would increase with the temperature increase, this may cause by the SNR of the data would increase with temperature increase.

3.2 Simultanues measurement of velocity and temperature

In this part, both of the heater and the contoured converging nozzle were used to generate high velocity flow at a desired temperature. Same with above temperature measurement, the thermocouple also placed at 12.7mm away from the nozzle exit. Recode both VIPA and online monitor data When the thermocouple reading become stable.

Figure.5 shows the mean of the nozzle flow velocity measurement along the laser direction. The total measurement probe is 28mm. The center axis of the nozzle located at 0mm. The ideal velocity at 0mm is 45m/s. This results shows the measurement taken at different locations provide a consistent velocity profile after the online correction by Etalon-base IRS system.

Figure.6 shows the standard deviation of this velocity measurement. Due to this measurement taken at a reletive low velocity, the shift in frequency space is not much. the precision was affected by the fitting strategy. If a better strategy could be brougt, the precision of the velocity at low velocity could improved. Because the focal at center is better then the edge, the standard deviation at the edge is higher then center. This is also can be overcomed by using different optical combanation.

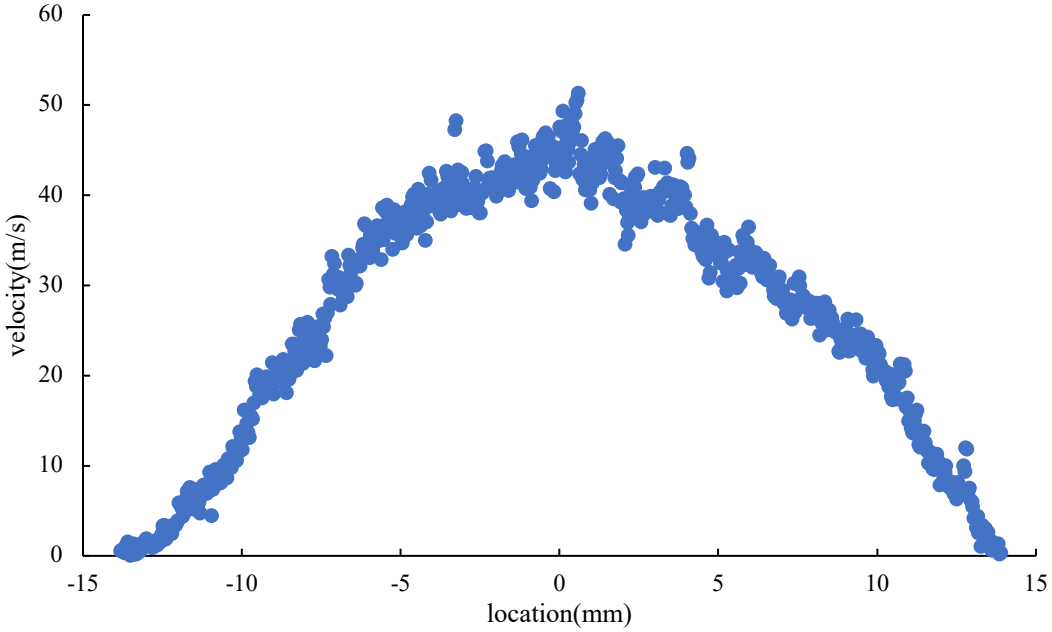

Figure.5 Velocity profile obtained in the flow at a location 2.8 cm downstream of exit.

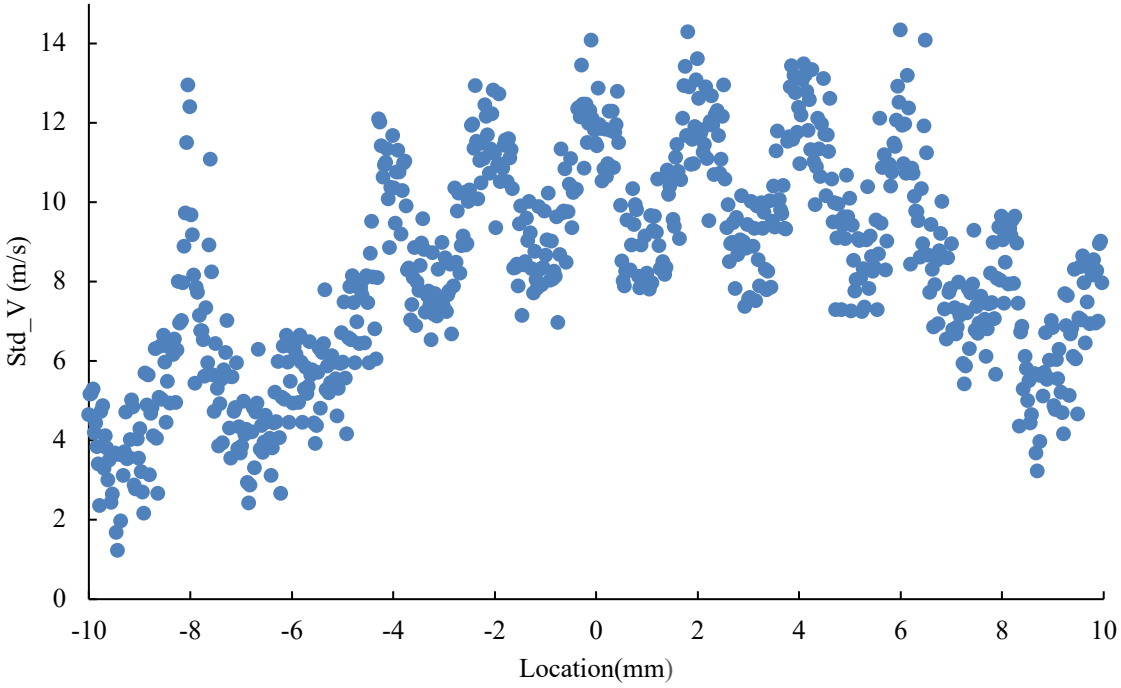

Figure.6 Velocity stand deviation in velocity measurement

Figure.7 shows the mean of the nozzle flow temperature measurement along the laser direction. As expected, the slope in tempearture at the interface between the flow and the surrounding air is larger in the lower part of the flow which is closer to the nozzle exit. The temperature profile is conisistant. The single-shot precision of the measurements, quantified by the standard deviation across the measurements from 50 images. The precision is ~10K in the center of the selected field of view (FOV) and increases to ~15K at the edges of FOV. This worsening of precision is due to the slight broadening of fringes and reduced intensity in the edge.

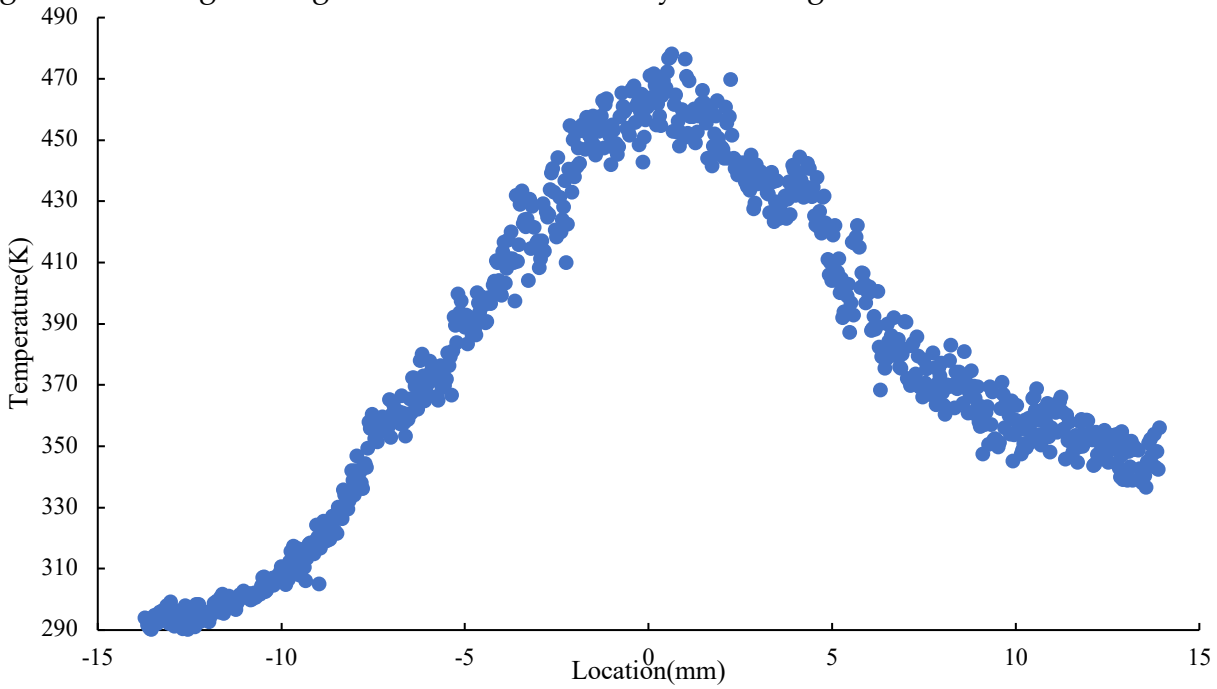

Figure.7 Temperature profile obtained in the flow at a location 2.8 cm downstream of exit.

4. Conclusions

A 1D interferometric Rayleigh scattering velocimetry and thermometry system has been developed and applied into the measurements of flow. The VIPA extended the interferometric Rayleigh scattering to 1D. Etalon used in this system to do the laser drift online correction. The proof of concept of using IRS is valided. The different fringers on one interferometric pattern acutually represent different measurement of same measurement probe, which is a effective way to do multiply measurement during one experiment. In simultanues measurement of flow velocity and temperature, the precision of velocity is 5m/s at center and 10m/s at the edge of each measurement probe. The precision of temperature in simultanues measurement is 10K at center and 15K at edge.

Acknowledgements

The research reported in this publication was supported by funding from King Abdullah University of Science and Technology (KAUST).

References

Bivolaru, D., Danehy, P., Lee, J., Gaffney, R., & Cutler, A. (2006). *Single-pulse multi-point multi-component interferometric Rayleigh scattering velocimeter.* Paper presented at the 44th AIAA Aerospace Sciences Meeting and Exhibit.

Boley, C., Desai, R. C., & Tenti, G. J. C. J. o. P. (1972). Kinetic models and Brillouin scattering in a molecular gas. *50*(18), 2158-2173.

Cutler, A. D., Rein, K., Roy, S., Danehy, P. M., & Jiang, N. (2020). 100-kHz Interferometric Rayleigh Scattering for multi-parameter flow measurements. *Optics Express, 28*(3), 3025-3040. doi:10.1364/OE.380934

Estevadeordal, J., Jiang, N., Cutler, A. D., Felver, J. J., Slipchenko, M. N., Danehy, P. M., . . . Roy, S. (2018). High-repetition-rate interferometric Rayleigh scattering for flow-velocity measurements. *Applied Physics B, 124*(3), 41. doi:10.1007/s00340-018-6908-y

Krishna, Y., Luo, X., & Magnotti, G. (2021). One-dimensional interferometric Rayleigh scattering velocimetry using a virtually imaged phased array. *Optics Letters, 46*(20), 5252-5255. doi:10.1364/OL.441913

Panda, J., & Seasholtz, R. (1999). *Velocity and temperature measurement in supersonic free jets using spectrally resolved Rayleigh scattering.* Paper presented at the 37th Aerospace Sciences Meeting and Exhibit.

Seasholtz, R. (1995). *Instantaneous 2D velocity and temperature measurements in high speed flows based on spectrally resolved molecular Rayleigh scattering.* Paper presented at the 33rd Aerospace Sciences Meeting and Exhibit.

Sheng, W., Si, J.-H., Jun, S., Hu, Z.-y., Ye, J.-f., & Liu, J.-R. J. O. E. (2017). Two-dimensional interferometric Rayleigh scattering velocimetry using multibeam probe laser. *56*(11), 111705.